SLAC-PUB-14982

An Experiment to Locate the Site of TeV Flaring in M87

D. E. Harris[1], F. Massaro[1,15], C. C. Cheung[2,3], D. Horns[4,5], M. Raue[4,5], Ł. Stawarz[5,6], S. Wagner[5,7], P. Colin[8,9], D. Mazin[9,10], R. Wagner[8,9], M. Beilicke[11,12], S. LeBohec[12,13], M. Hui[12,13], and R. Mukherjee[12,14]

ABSTRACT

We describe a Chandra X-ray Target of Opportunity project designed to isolate the site of TeV flaring in the radio galaxy M87. To date, we have triggered the Chandra observations only once (2010 April) and by the time of the first of our 9 observations, the TeV flare had ended. However, we found that the X-ray intensity of the unresolved nucleus was at an elevated level for our first observation. Of the more than 60 Chandra observations we have made of the M87 jet covering 9 years, the nucleus was measured at a comparably high level only 3 times. Two of these occasions can be associated with TeV flaring, and at the time of the third event, there were no TeV monitoring activities. From the rapidity of the intensity drop of the nucleus, we infer that the size of the emitting region is of order a few light days $\times$ the unknown beaming factor; comparable to the same sort of estimate for the TeV emitting region. We also find evidence of spectral evolution in the X-ray band which seems consistent with radiative losses affecting the non-thermal population of the emitting electrons within the unresolved nucleus.

Subject headings: galaxies: active—galaxies: individual(M87)—galaxies: jets— X-rays: general

1. Introduction: The Problem

Although the radio galaxy M87 is normally a weak source at TeV energies, occasionally there is flaring activity which lasts from a few days up to a week or two. During these times, the observed intensity can peak at $\geq 10\%$ Crab. To date there have been 3 well documented flarings:

- 2005 April - H.E.S.S. found variable TeV emission with typical timescales of a few days (Aharonian et al. 2006). Since this event coincided with the peak of the giant flare (radio/UV/X-ray) from the knot HST-1 which lies at 0.86″ (60pc in projec-

[1]SAO, 60 Garden St., Cambridge, MA 02138

[2]National Research Council Research Associate, National Academy of Sciences, Washington, DC 20001, resident at Naval Research Laboratory, Washington, DC 20375, USA

[3]a member of the Fermi-LAT collaboration

[4]University of Hamburg, Institute for Experimental Physics, Luruper Chaussee 149, D-22761 Hamburg, Germany

[5]a member of the H.E.S.S. collaboration

[6]Institute of Space and Astronautical Science, JAXA, 3-1-1 Yoshinodai, Sagamihara, Kanagawa, 229-8510, Japan and Astronomical Observatory, Jagellonian University, ul. Orla 171, 30-244 Kraków, Poland

[7]Landessternwarte Heidelberg-Koenigstuhl, 69117 Heidelberg Germany

[8]Max-Planck-Institut für Physik, D-80805 München, Germany

[9]a member of the MAGIC collaboration

[10]IFAE, Edifici Cn., Campus UAB, E-08193 Bellaterra, Spain

[11]Washington University in St.Louis, Campus Box 1105, 1 Brookings Drive, St.Louis, MO 63130

[12]a member of the VERITAS collaboration

[13]University of Utah, Department of Physics 115 South 1400 East, Salt-Lake-City, UT 84112-0830

[14]Barnard College, Physics & Astronomy, New York NY 10027

[15]SLAC National Laboratory and Kavli Institute for Particle Astrophysics and Cosmology, 2575 Sand Hill Road, Menlo Park, CA 94025

KIPAC, SLAC National Accelerator Laboratory, 2575 Sand Hill Road, Menlo Park, CA 94025

Work supported in part by US Department of Energy contract DE-AC02-76SF00515.

tion) from the nucleus of M87, there has been an on-going debate as to whether the TeV emission originated near the supermassive black hole in the nucleus or from HST-1 (Harris et al. (2009), and references therein).

- 2008 Feb - A second flaring event which lasted for almost two weeks was observed by H.E.S.S., MAGIC, and VERITAS. By chance, a series of VLBA observations was underway by R. C. Walker at 43 GHz: the milliarcsec nucleus progressively brightened (Acciari et al. 2009). One of our standard Chandra X-ray monitoring observations occurred a few days after the TeV flaring and we found that the nucleus was brighter than usual whereas HST-1 maintained a comparatively constant intensity. See also Acciari et al. (2010).

- 2010 Apr - This event was observed by H.E.S.S., MAGIC, and VERITAS (Ong & Mariotti 2010). Once the reality of the flaring was established, a Chandra target-of-opportunity (ToO) was triggered and these results are the subject of this paper. Although HST-1 has declined from its peak intensity in 2005 to levels similar to those in 2000, the nuclear X-ray emission was at a somewhat higher level than usual. However, no activity at 43 GHz was detected. For more details, see Abramowski et al. (2011).

From the TeV variability timescale, it is deduced that the TeV emitting region is of the order of a light day times δ, the unknown Doppler beaming factor (Abramowski et al. 2011). Although we have not found such short timescale variability in the X-rays from HST–1, the nucleus has a somewhat shorter timescale for variability than the 20 days of HST-1 (Harris et al. 2009).

So the open question is, can we determine the site of the TeV flaring by identifying common features in the lightcurves at TeV and at X-rays?

At a distance of 16 Mpc, the angular scale for M87 is 77pc/arcsec. Spectral indices are defined by flux density, $S_\nu \propto \nu^{-\alpha}$.

2. The Experiment

The basic idea for our Chandra ToO program on M87 is to trigger a series of observations when the TeV exhibited a level of $\geq$7% Crab. With luck, we had hoped that the X-ray light curve of either the nucleus or HST-1 would divulge some feature that would correspond to the TeV excursions. The main problem for this experiment is the brevity of the TeV flaring compared to the time it takes for Chandra mission planning to alter the observing schedule and upload a revised observing schedule.

Our strategy was to make an initial 5 ks Chandra observation as soon as possible after receiving the TeV trigger, and then to follow the first with 4 more 5ks observations spaced at intervals of between 1.5 and 3 days. We then had 4 more observations, the first of which would start at the beginning of the next dark of the moon fortnight, and these would be spaced by 3$\pm$1 days. The lunar constraint was imposed since it would make little sense to discover discrete features in the X-ray light curves around the full moon when TeV observations are difficult or impossible.

On Friday, 2010 April 9 the trigger level was realized (see Ong & Mariotti (2010)) and our first observation was late in the day on Sunday (April 11). Unfortunately, the final elevated TeV level occurred on Saturday night; by Sunday night when we obtained the first Chandra observation, the TeV flaring was over.

3. The Observations & Data Reduction

In Table 1 we list the particulars of our Chandra observations. In addition to the 9 observations of this ToO in 2010 April and May, we include a reanalysis of an observation (labeled 'Zh' in previous papers) obtained on 2008 Feb 16.5, which was 3 days after the final activity (Feb 13) of an earlier TeV flaring event (see §1).

3.1. Data Processing

Our data processing of M87 5 ks observations (we have accumulated over 60 of these during the years 2002-2009; (Harris et al. 2009; Acciari et al. 2010)) has purposefully remained essentially unchanged except for the changes made to the CALDB. In brief, we check for high background levels, remove pixel randomization (the in-

TABLE 1
CHANDRA OBSERVATIONS

Name	OBSID	Start Time (UT)	Live Time (sec)
Zhed	8577	2008-02-16T11:30:12	4659
eda1	11512	2010-04-11T21:14:39	4699
eda2	11513	2010-04-13T14:16:43	4703
eda3	11514	2010-04-15T20:32:42	4529
eda4	11515	2010-04-17T21:47:42	4699
eda5	11516	2010-04-20T13:20:52	4707
eda6	11517	2010-05-05T19:25:21	4703
eda7	11518	2010-05-09T02:39:49	4402
eda8	11519	2010-05-11T11:17:03	4706
eda9	11520	2010-05-14T09:04:59	4595

NOTE.—The first column provides a label for each observation. 'Zhed' combines the previous designation (Zh) with 'ed' which is short for EDSER, the subpixel repositioning algorithm used for all our data in this paper. 'eda' is a compression of 'EDSER April'.

tentional degradation of image quality by adding a random number to the pixel location of each event; this process was a part of the pipeline processing until quite recently), register the X-ray event file by changing the values of appropriate keywords in the fits header so as to align the X-ray nucleus with the radio nucleus, and then construct fluxmaps regridded to one tenth of the native ACIS pixel size (i.e. pixels size changes from 0.492″ to 0.0492″). This last step is done for the soft band (0.2-0.75 keV), the medium band (0.75-2 keV), and the hard band (2-6 keV). Because of severe pileup[1] for the knot HST-1 during its high intensity flaring in 2005, we forsook cgs units (the fluxmaps) and instead made our primary intensity measurement in terms of keV/s. This photometry was performed using the event 1 file[2] with no grade filtering, and integrated from 0.2 keV up to whatever energy was required to recover essentially all the events associated with a given feature. In the rest of this paper, it is important to distinguish between counts per sec (used primarily in dealing with evaluation of pileup) and keV/s, which is the sum of each event multiplied by its energy. Since most photons are of order 1 keV, the magnitudes of these two observational parameters are quite similar. Further details of our processing methods can be found in Papers I, III, and V of our series (Harris et al. 2003, 2006, 2009, respectively).

For the current effort we have altered our procedures in a few particulars. First we changed the 'bad pixel' routine to the 'hot pix' recently released in CIAO. More importantly however, we used *acis_process_events* to apply the EDSER algorithm[3] in place of the removal of pixel randomization. In various tests, we found that data processed with EDSER produce a more narrow point-spread function and consequently a higher peak intensity. While not a drastic improvement, it is sufficiently good so as to be a valuable asset in separating the nucleus from HST-1 (separated by

[1]The term 'pileup' is used for CCD detectors to describe the situation of a detected event consisting of two or more different photons which happened to arrive during the same frame integration time and close to the same location on the detector.

[2]The event 1 file contains all the events; the event 2 file has been filtered for standard grades and also filtered for good time intervals.

[3]The term 'EDSER' stands for "energy dependent sub-pixel event repositioning": it is an algorithm recently included in CIAO and the pipeline processing which uses the charge distribution within a 3x3 pixel region to refine the assumed location of the incoming photon in detector coordinates.

0.86″). An example (our first observation, 'eda1') is shown in fig. 1, which will also serve to illustrate the apertures for photometry.

3.2. Examination of Pileup

Before attempting to evaluate the characteristics of the nuclear data that exceed 1 kev/s, it behooves us to consider the effects of pileup in the ACIS CCD's.

Although we have had to deal with severe pileup for the high intensity of the knot HST-1 in 2005, we generally considered levels of ≤1 keV/s as weak enough so that pileup could be ignored. However, in the present case, we realize that even if a minority of incoming photons arrived during a frame time with another photon, the resulting events would masquerade as single photons of higher energy, distorting the spectral distribution. Therefore, to understand the effects of mild pileup, we examined 3 parameters indicative of pileup, and use the countrate of the event 1 file as our independent variable.

The first is the ratio of the measured intensities (keV/s) in the event 2 file to that in the event 1 file. We time filtered the event 1 file but did not filter for standard grades since we wanted to recover those events which suffered grade migration,[4] a common symptom of pileup. For knot A which is slightly resolved and not expected to suffer pileup, the intensity is about 0.2 c/s (0.08 counts per frame since we always use 0.4s frame time). Values for the ratio keV/s(evt2/evt1) range between 0.95 and 0.98 for the 10 observations of Table 1. For knot D which has an intensity roughly half that of knot A, the observed ratios go from 0.96 to 0.99.

For the 9 observations of 2010, HST-1 had an intensity between 0.25 and 0.28 c/s and the observed ratio ranged from 0.89 to 0.95. In 2008 Feb the intensity was 0.82 c/s and the ratio was 0.79. For the nucleus, the two intensities greater than 1 keV/s had ratios of 0.78 and 0.85 whereas the lower intensity observations ranged from 0.91 to

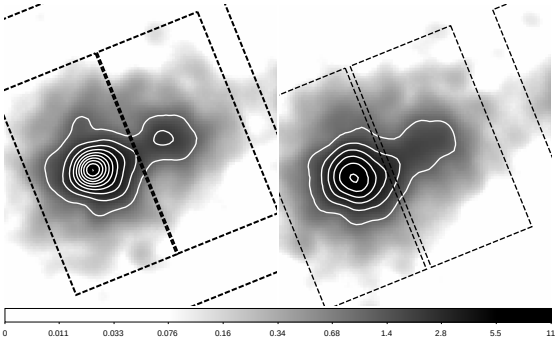

Fig. 1.— A comparison of EDSER (left) vs. 'pixel randomization removed' (right) processing for the first observation of 2010 April ('eda1'). The nucleus and HST-1 (the feature towards the NW) are separated by 0.86″. Each image has been rebinned to 1/16 native ACIS pixel and smoothed with a Gaussian of FWHM = 0.22″. The grayscales are logarithmic but the contours are linear. For the left panel (EDSER) the peak intensity is 10.648 counts/pixel and the contours are set to 10, 20, 30, ... 100%. The right panel has peak intensity of 6.59 counts/pixel and, for illustrative purposes, we have applied the same (absolute) contour levels, i.e. 1.07, 2.15, 3.23, ... 6.47 (cts/pix). As described in the text. our standard rectangular photometric regions for the nucleus and HST-1 were found to be slightly misplaced when judged with an EDSER image. In the right panel we show the standard rectangles and in the left panel are the slightly shifted rectangles.

[4]The term 'grade migration' describes what happens when a single event consists of more than one photon. Many of these events (because the charge of the second or third photon is positioned at a different location) will cause the filtering software to label these as 'bad grades' (e.g. cosmic rays), and when grade filtering between event 1 and event 2 files occurs, these events will be rejected.

0.93 for the ratio.

The loss of detected energy passing from event 1 to event 2 is reflected in the loss of detected events caused by grade migration. In fig. 2 we show this effect.

Another indicator of pileup is the average energy of all detected events. Although $< E >$ is ambiguous since it will increase if the intrinsic source spectrum hardens, if coupled with detectable grade migration, it is a necessary consequence of pileup. Not only will the energy of piled events be much larger than the average of unpiled events, but the average energy will be augmented because there are fewer events than there should be owing to the doubling up of piling. This predicted effect is present in our data: the mean energies for the nucleus for the 8 observations of intensity < 1 keV/s range between 1.38 and 1.53 keV while for Zhed it is 1.78 and for eda1 it is 1.57. Similarly, $< E >$(Zhed) for HST-1 is 1.47 keV compared to the 2010 values which range between 1.15 and 1.28.

We have also used PIMMS[5] to estimate pileup. Specifying the input as Chandra c/s with frame time 0.4s, a power law with photon index = 2, and absorption by a column density of $N_h = 4 \times 10^{20}\mathrm{cm}^{-2}$; we constructed a 'look-up' table of input (photons per sec arriving at the detector) and output c/s, which is the countrate of the unpiled photons. We calculated the total event rate from the expression:

$$\text{observed(evt1 c/s)} = \frac{PIMMS(output)c/s}{1-Fp}$$

where Fp is the fractional pileup reported by PIMMS and is defined as the number of piled events divided by the total number of events. We use the observed event rate from the event 1 file which has been time filtered but not grade filtered because PIMMS does not accommodate corrections for grade migration. In this way we can estimate the inferred counting rate from each component in the absence of pileup. Relevant numbers are given in Tables 2 (nucleus) & 3 (HST-1), and it is clear that even with a frame time of 0.4s, pileup will significantly affect most source parameters except for the intensity in keV/s, which was specifically designed to circumvent first order

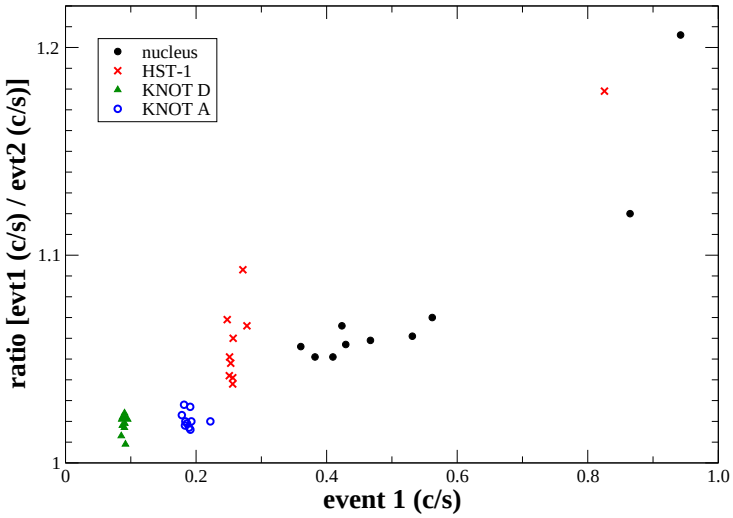

Fig. 2.— The ratio of event 1 countrate to that from the event 2 file. When pileup becomes significant, the event 2 countrate decreases relative to the event 1 countrate as more and more events are rejected by the standard grade filtering. The data point for the nucleus in 2008 Feb. has the largest ratio and the largest event 1 intensity. The other nuclear point at the right in the plot is from the eda1 observation, our first after the TeV flaring of 2010 April. HST-1 had a larger intensity (and hence a larger ratio) in 2008 than in 2010. The data for knots D and A have ratios close to unity and are essentially free of pileup effects. The fact that not all the data for the nucleus and HST-1 lie on a single curve is most likely caused by an interaction between these two components (e.g. a mild case of 'Eat Thy Neighbour', as described in Harris et al. (2009)).

[5]http://heasarc.gsfc.nasa.gov/Tools/w3pimms.html

TABLE 2

X-RAY INTENSITIES, PILEUP PARAMETERS, AND SPECTRAL INDICES FOR THE NUCLEUS.

Observation	Intensity [a] (keV/s)	Event2 (c/s)	Event1 (c/s)	PIMMS [b] (c/s)	Fractional [c] Pileup	α_x
Zhed	1.692±0.026	0.781	0.942	1.11	0.16	0.87±0.05
eda1	1.365±0.021	0.772	0.865	1.01	0.15	0.92±0.04
eda2	0.774±0.015	0.525	0.562	0.62	0.10	1.19±0.06
eda3	0.641±0.015	0.406	0.429	0.46	0.07	1.02±0.07
eda4	0.669±0.014	0.441	0.467	0.50	0.08	1.13±0.07
eda5	0.650±0.015	0.397	0.423	0.45	0.07	1.06±0.07
eda6	0.767±0.015	0.501	0.531	0.58	0.09	1.05±0.05
eda7	0.577±0.014	0.390	0.410	0.45	0.07	1.12±0.07
eda8	0.541±0.013	0.364	0.382	0.41	0.06	1.06±0.07
eda9	0.517±0.013	0.341	0.360	0.38	0.06	1.03±0.08

NOTE.—The statistical uncertainties for the countrates are of order a few percent

[a]The ± values are the statistical uncertainties derived from the corresponding countrates.

[b]The PIMMS countrate attempts to estimate the rate at which photons are arriving at the detector, i.e. source count rate in the absence of pileup.

[c]The fractional pileup from PIMMS, defined as the ratio of piled events to total events.

TABLE 3

X-RAY INTENSITIES, PILEUP PARAMETERS, AND SPECTRAL INDICES FOR HST-1.

Observation	Intensity [a] (keV/s)	Event2 (c/s)	Event1 (c/s)	PIMMS [b] (c/s)	Fractional [c] Pileup	α_x
Zhed	1.212±0.020	0.700	0.826	0.95	0.14	1.16±0.05
eda1	0.348±0.010	0.249	0.272	0.28	0.04	1.32±0.10
eda2	0.309±0.009	0.232	0.248	0.25	0.04	1.51±0.12
eda3	0.292±0.009	0.242	0.253	0.26	0.04	1.53±0.12
eda4	0.316±0.009	0.246	0.256	0.26	0.04	1.67±0.12
eda5	0.343±0.009	0.261	0.278	0.29	0.04	1.49±0.11
eda6	0.308±0.009	0.242	0.257	0.26	0.04	1.56±0.12
eda7	0.306±0.009	0.239	0.251	0.26	0.04	1.52±0.13
eda8	0.312±0.009	0.241	0.251	0.26	0.04	1.56±0.11
eda9	0.301±0.009	0.247	0.256	0.26	0.04	1.56±0.11

NOTE.—The statistical uncertainties for the countrates are of order a few percent

[a]The ± values are the statistical uncertainties derived from the corresponding countrates.

[b]The PIMMS countrate attempts to estimate the rate at which photons are arriving at the detector, i.e. source count rate in the absence of pileup.

[c]The fractional pileup from PIMMS, defined as the ratio of piled events to total events.

pileup problems.

3.3. Photometry

X-ray intensities were measured using the rectangular apertures defined previously. The keV/s values are given in Tables 2 & 3, and plotted in fig. 3. We do not include tabular data for knots D and A since they are not viable candidates for the site of flaring TeV emission and pileup is negligible for both: knot D has a much smaller counting rate than the nucleus and HST-1, whereas knot A is resolved. The data for these two knots are included in fig. 3 as 'control features'; any intrinsic variability in these two knots is at a much lower level than for the nucleus and HST-1.

4. Discussion

If the predominant emission mechanism for the nuclear X-rays is synchrotron emission as it is for HST-1, then there must be a sizable population of high energy relativistic electrons whose IC emission will be in the TeV range (Harris et al. 2009). In fig. 3 we show the light curves for the nucleus, HST-1, knots D and A. Note the high level of the nucleus at our first observation and the sharp drop to more normal levels by the time of the second observation.

Although our experiment failed to isolate discernable features in the X-ray light curves corresponding to TeV features, it yielded tantalizing hints that we most likely witnessed the tail end of a period of X-ray flaring associated with the TeV flaring. The intriguing question is what we might have seen if Chandra observations had begun a few days earlier. If the slope of the nuclear light curve before our first observation was similar to that between the first two observations, the X-ray intensity of the nucleus during the TeV flaring would have been remarkable.

During our 8 years of monitoring the M87 jet with Chandra (Harris et al. 2009; Acciari et al. 2010), the nuclear emission has seldom been larger than 1 keV/s: on two occasions (2008 Feb 16 and 2010 Apr 11) these levels were in close proximity to TeV flaring. A third time (2006 Jun 28), there was no TeV coverage, and for the 2005 April TeV flaring, our data are not reliable because of second order pileup effects associated with HST-1.

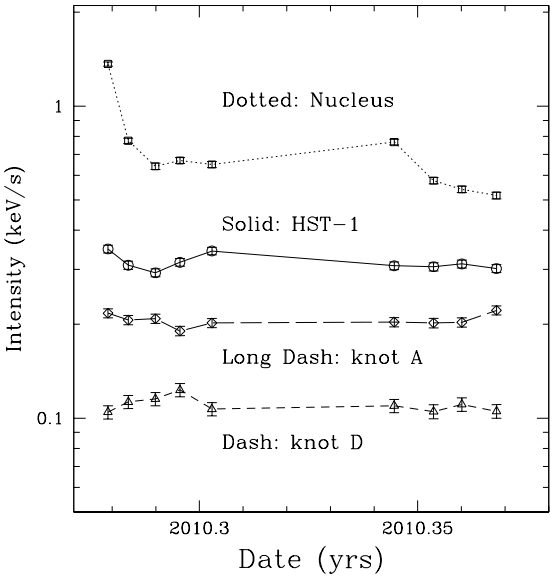

Fig. 3.— The light curves for (top to bottom) the nucleus, HST-1, knot A, and knot D. Intensity units are keV/s and are derived from the event 1 file with no grade filtering. The first observation was obtained on 2011 April 11; the last on May 14.

4.1. The X-ray - TeV Connection

For the case of HST-1, we became convinced that the huge flare of 2005 could be described by a broadband synchrotron emission from the radio to the X-rays in an equipartition field of ≈1mG (Papers I, III, & V). With the presence of electrons with Lorentz factors, $\gamma \approx 10^7$, we showed that such a source would be expected to produce inverse Compton (IC) emission in the TeV range from ambient photons (Paper IV). Moreover, although it is probable that expansion losses were operative, there were time intervals which manifest the signature of energy-dependent radiative losses and the decay times were consistent with a 1mG field (Paper V).

When we consider the emission from the unresolved (by Chandra) nuclear component, we cannot devise a complete scenario because there are so many unknowns: primarily the source size and the broadband nature of the emission. It may be the case that the operative field strength is significantly larger than that of HST-1, the emitting volume may be much smaller, and the beaming factor could be quite different (either larger or smaller than the estimate of $\delta \approx 5$ for HST-1; Perlman et al. (2011)). In Abramowski et al. (2011) it is clearly shown that the evidence at hand provides mixed results when attempting to show broadband emission associated with TeV flaring. While one can argue that the X-ray flux observed from the nucleus is always a bit larger than normal at the time of TeV flaring, the 43 GHz 'activity' from the milliarcsec core appeared on one occasion but was absent on another.

One might, in fact, propose that the major acceleration mechanism could be reconnection rather than shock acceleration, and therefore, there could well be quite a different distribution of relativistic electrons from the broken power law from low values of γ up to 10^7 or 10^8 suggested to explain the broadband emission from HST-1. If such were to be the case, there is no a priori reason to expect that a particular band will show anomalous emission directly associated with the TeV flaring. With this caveat in mind, we will now argue that there is, in fact, circumstantial evidence for X-ray emission from the nucleus of M87 which is associated with TeV flaring.

4.2. The 2010 April X-ray Event

For the nucleus, the spectral differences we have measured between the first and remaining observations are in the same direction as would be expected from the change in pileup fraction.

The drop in the nuclear intensity between our first two observations (separated by 1.68 days) permits us to measure the fractional change per day, '*fpd*' (see Paper V where *fpy* - 'fractional change per year' was introduced) and compare its value to the historical behavior during 8 years of monitoring. Typically, the largest values found previously for the nucleus were *fpy* ≈50, corresponding to an *fpd* value of *fpy*/365 ≈0.137 (both positive and negative *fpy's* of this magnitude were observed). The *fpd* (or *fpy*) formulae are:

$$fpd = (I_2 - I_1)/(I_i \Delta\ t)$$

$$\sigma(fpd) = \frac{1}{\Delta(t)} \times \frac{I_j}{I_i} \times \sqrt{(\frac{\sigma_1}{I_1})^2\ +\ (\frac{\sigma_2}{I_2})^2}$$

where I_1 and I_2 are successive intensities, $\Delta\ t = (t_2 - t_1)$, and i=1, j=2 when the source is getting brighter and i=2, j=1 when the intensity is dropping. The time it would take to change the intensity by a factor of two for an observed value of *fpd* is 1/*fpd*.

The calculated values of *fpd* (between eda1 and eda2) for various intensity measurements are −0.454±0.027 for keV/s; −0.150±0.041 for the soft flux; −0.266±0.030 for the medium flux; and −0.643±0.071 for the hard flux. While it would be useful to know if the hard flux was dropping faster than the soft flux, the apparent effect could be caused, in whole or in part, by the reduction of the pileup fraction between eda1 and eda2.

To estimate the spectral distribution of the incident photons (i.e. what we would have observed in the absence of pileup), we adopted the rather extreme assumption that all the piled events ended up in the hard band, and assumed that of the arriving photons which eventually piled, 1/3 came from the soft band and 2/3 came from the medium band. This is 'extreme' because some of the piled events will actually end up in the medium band and because some fraction of the piled events will actually consist of 3 photons rather than just two. Taking the observed count rates from the event 1 file (i.e. no grade filtering) we were then able to estimate the *incident* count rates for each band

for both eda1 and eda2. It is then a simple matter to calculate *fpd* values but the uncertainties will be dominated by errors in assuming the particulars of the pileup. Therefore, we have calculated the uncertainties for the observed *fpd*, but not for the assumed incident count rates: the results are presented in Table 4.

The 'exercise' of assuming how the piled events are distributed among the energy bands is just to get some rough idea to differentiate between pileup effects and intrinsic attributes. *Fpd* is a good measure of the rate of decay of intensity and we take the decrease of *fpd*(incident) moving from soft to hard as evidence for the presence of energy-dependent radiative losses. The fact that the spectral index for eda2 is the largest among all our observations even though the intensity is second only to eda1, is further evidence that pileup is not the dominant factor for the *fpd* dependency on energy.

Generally speaking, the most plausible mechanisms for a drop of intensity for a non-thermal source is either expansion (which has no first order effect on the spectral shape of the electron energy distribution) or the radiative cooling with the energy loss rate increasing with increasing energies of the radiating particles (for example as $\propto E^2$ in the case of the synchrotron and inverse Compton emission). [6] Although the dimming of radio emission from parsec scale knots is often ascribed to expansion, when dealing with high energy emissions which must come from electrons with much greater energies than those producing radio emission, energy-dependent radiative losses are much more likely to contribute to the dimming, with or without expansion.

From the general magnitude of *fpd* values we may also infer that the light travel time across the X-ray emitting region is limited to a few days, thus being consistent with estimates of the size of the TeV flaring regions deduced by the timescale of TeV variability (Aharonian et al. 2006; Abramowski et al. 2011).

Although our experiment did not succeed in isolating similar features in the X-ray and TeV light curves, we find evidence that supports the notion that there was concomitant flaring in the X-rays, and we witnessed the last phase of that flaring.

K. Mukai provided helpful information and advice on the implementation of pileup in PIMMS. We thank R. C. Walker for helpful suggestions on the manuscript. F. Massaro acknowledges the Fondazione Angelo Della Riccia for the grant awarded him to support his research at SAO during 2011 and the Foundation BLANCEFLOR Boncompagni-Ludovisi, n'ee Bildt for the grant awarded him in 2010 to support his research. We thank the *Chandra* mission planning team and the director's office for their tireless efforts to reschedule target of opportunity observations. The anonymous referee is thanked for his useful comments. The work at SAO was supported by NASA grant GO0-11120X.

Facilities: Chandra.

REFERENCES

Abramowski, A. et al. 2011, submitted to the ApJ

Aharonian, F. et al. 2006 Science 314, 1424

Acciari, V. A. et al. 2009, Science 325, 444

Acciari, V. A. et al. 2010, ApJ 716, 819

Harris, D. E., Biretta, J. A., Junor, W., Perlman, E. S., Sparks, W. B., & Wilson, A. S. 2003 ApJ 586, L41

Harris, D. E., Cheung, C. C., Biretta, J. A., Sparks, W. B., Junor, W., Perlman, E. S., & Wilson, A. S. 2006 ApJ 640, 211

Harris, D. E., Cheung, C. C., Stawarz, L., Biretta, J. A., & Perlman, E. S. 2009 ApJ 699, 305

Ong, R.A., & Mariotti, M., 2010, The Astronomer's Telegram, 2541, 1

Perlman, E. S., Adams, S. C., Cara, M., Bourque, M., Harris, D. E., Madrid, J. P., Simons, R. C., Clausen-Brown, E., Cheung, C. C., Stawarz, L., Georganopolous, M., Sparks, W. B., & Biretta, J. A. 2011 ApJ (in press, arXiv:1109.6252)

[6] Caveat: simple expansion can produce a similar spectral signature if there is a break in the power law spectrum or the spectrum is curved (Harris et al. 2009).

This 2-column preprint was prepared with the AAS LaTeX macros v5.2.

TABLE 4
THE X-RAY INTENSITY DECAY OF THE NUCLEUS

	Soft 0.2-0.75keV	Medium 0.75-2keV	Hard 2-6keV	Total 0.2-6keV
eda1(observed) c/s	0.167	0.498	0.192	0.857
eda2(observed) c/s	0.139	0.335	0.085	0.559
fpd(observed)[a]	−0.122	−0.288	−0.750	−0.317
σ(fpd-obs)[b]	0.038	0.029	0.081	0.023
eda1(inferred) c/s	0.257	0.678	0.055	0.991
eda2(inferred) c/s	0.179	0.405	0.028	0.614
fpd(inferred)[a]	−0.262	−0.400	−0.587	−0.366

NOTE.—The observed values come from the event 1 file (no grade filtering). The 'inferred' entries are estimated incident count rates (i.e. in the absence of pileup).

[a] *fpd* is the fractional change per day. The values quoted in §4.2 are based on flux maps; here in the table they are based on count rate.

[b] σ(fpd-obs) is an estimate of the uncertainty of *fpd*, calculated in the standard fashion ($\sqrt{N}$/N, where N is the number of events in the appropriate energy band).